

## Solvatochromic behaviour of new donor-acceptor oligothiophenes

Francesca D'Anna,<sup>\*a</sup> Fabiana Pandolfi,<sup>b</sup> Daniele Rocco,<sup>b</sup> Salvatore Marullo,<sup>a</sup> Marta Feroci<sup>b</sup> and Leonardo Mattiello<sup>\*b</sup>

Received 00th January 20xx,  
Accepted 00th January 20xx

DOI: 10.1039/x0xx00000x

Oligothiophene derivatives play a central role in the formulation of materials used in devices in the field of organic electronics. In this work we report the results of the study of UV-Vis absorption and fluorescence spectra, in several solvents, of a series of oligothiophenes recently synthesized in our laboratory. The studied oligothiophenes present different structures due to several factors: the Donor-Acceptor (D-A) or Acceptor-Donor-Acceptor (A-D-A) architecture; the number of thiophene rings in the backbone (ranging from three to eight); the number and position of solubilizing octyl chains in the backbone, and the type of acceptor moieties (from Knoevenagel condensation either with ethyl cyanoacetate or 3-ethylrhodanine). Since solvents with different polarities were adopted, we provide a detailed analysis on the observed positive and negative solvatochromism effects depending on the symmetry of the oligomers, the lengths of the backbones and the kind of acceptors adopted. Moreover, an electrochemical synthesis of a new donor-acceptor oligothiophene (which can be assumed as a model compound) by anodic dimerization is reported, along with the voltammetric analysis of the obtained product.

### Introduction

Organic semiconductors represent the key element on which the concept of Organic Electronics is based.<sup>1,2</sup>

Among them, the most important role is certainly that played by thiophene derivatives, both in polymeric and oligomeric form.<sup>3</sup>

A large number of these compounds can be found, for example, in organic light-emitting diodes,<sup>4-7</sup> organic thin film transistors,<sup>8,9</sup> organic solar cells,<sup>10-15</sup> organic photodetectors.<sup>16</sup> Thiophene-based materials have excellent charge transport properties, however, oligothiophenes, compared to the more commonly used polythiophenes, have undeniable advantages due to the possibility of being synthesized with exactly defined structures, with greater purity and cost-effectiveness. We have synthesized oligothiophenes with different number of monomer units based on donor-acceptor (D-A) and acceptor-donor-acceptor (A-D-A) architectures, using different donor cores and acceptor end groups. The syntheses were carried out not only by classical organic chemistry but also by means of anodic dimerizations; in this way it has been shown that, in addition to providing important information such as HOMO and LUMO energy levels, electrochemistry is also useful for shortening and simplifying otherwise long synthetic processes.

To have insights into some physico-chemical properties of our oligothiophenes, especially regarding their use in optoelectronic devices, solvatochromic studies can be carried out.

In general, solvatochromism regards the effect of the probe surrounding (solvent) on its spectroscopic properties.<sup>19</sup>

In particular, during energy absorption, the electrons pass from the ground state to the excited state, and, after possible non radiative energy dissipation, they return to the ground state with energy emission. The solvent (probe surrounding) can influence differentially both ground and excited states, leading to a bathochromic or a hypsochromic shift with respect to a reference solvent. The structure of our oligothiophenes (donor, acceptor,  $\pi$ -bridge) allows for both dipole and dispersion interactions, possibly leading to interactions of different extent between solvent and ground state molecule and excited state one varying the nature and thus the physico-chemical properties of the solvent.

As the absorption and emission wavelengths of compounds used in optoelectronics (both pure and in solution) are highly important, a solvatochromic study prior to their use in real devices is of crucial importance.

### Experimental

#### Materials and methods

Compounds **T2T**, **BT2T**, **T1N**, **T2N**, **BT1N**, **BT1C**, **BT2N**, **BT2C**, **BT4N**, **BT6N**, **D8N** were synthesized and characterized as recently reported.<sup>17,18</sup> Thin layer chromatography was carried out using Alugram SIL G/UV254 plates and visualized under UV

<sup>a</sup> Università degli Studi di Palermo, Dipartimento di Scienze e Tecnologie Biologiche Chimiche e Farmaceutiche, Viale delle Scienze, Ed. 17, 90128, Palermo (Italia).

<sup>b</sup> Sapienza Università di Roma, Dipartimento di Scienze di Base e Applicate per l'Ingegneria, Via del Castro Laurenziano 7, 00161, Roma (Italia).

Electronic Supplementary Information (ESI) available: absorption UV-Vis spectra; emission spectra; plots  $\lambda_{\text{obs}}$  vs  $E_T(30)$ ; plots  $\lambda_{\text{em}}$  vs  $E_T(30)$ ; Lippert-Mataga equation plots. See DOI: 10.1039/x0xx00000x

light (at 254 and/or 365 nm). Flash chromatography was carried out using Silica Gel 60 (0.04–0.063 mm).  $^1\text{H}$  and  $^{13}\text{C}$ -NMR spectra were acquired on a Bruker AVANCE-400 spectrometer at 9.4 T, in  $\text{CDCl}_3$  at 27 °C. The residual signals for the NMR solvent ( $\text{CDCl}_3$ ) are 77.16 ppm ( $^{13}\text{C}$ ) and 7.27 ppm ( $^1\text{H}$ ); the following abbreviations have been used for NMR assignment: s for singlet, d for doublet, t for triplet, q for quartet, quint for quintet and m for multiplet.

Voltammetric measurements were performed using an Amel System 5000 electrochemical workstation. Measurements were carried out under a nitrogen atmosphere in a conventional three electrode cell with a 492/GC/3 Amel microelectrode as the working electrode, a Pt wire as the counter electrode and a modified saturated calomel electrode as reference electrode (mSCE: SCE with organic solvent junction; the standard redox potential of the ferrocenium/ferrocene system is  $E^\circ(\text{Fc}^+/\text{Fc}) = +0.52 \text{ V vs SCE}$ ). All experiments were carried out at 25 °C, in anhydrous dichloromethane (DCM) with 0.1 M tetrabutylammonium tetrafluoroborate ( $\text{Bu}_4\text{NBF}_4$ ), the concentration of the substrate was  $1 \times 10^{-2} \text{ M}$ .

### Chemical and electrochemical syntheses

#### Anodic Dimerization of ethyl 2-cyano-3-(3,3'-dioctyl-[2,2':5',2''-terthiophene]-5-yl)acrylate (T1N)

The electrolysis was carried out under nitrogen atmosphere at room temperature at constant potential of +1.4 V (vs mSCE), using an Amel Model 552 potentiostat equipped with an Amel Model 731 integrator. Pt spirals (apparent area 0.8  $\text{cm}^2$ ) were used as both cathode and anode. Catholyte (5 mL  $\text{CH}_2\text{Cl}_2$ - $\text{Bu}_4\text{NBF}_4$  0.1 M) and anolyte (5 mL  $\text{CH}_2\text{Cl}_2$ - $\text{Bu}_4\text{NBF}_4$  0.1 M, containing 0.28 mmol of T1N) were separated through a G-3 glass septum filled up with a layer of gel (i.e., methyl cellulose 0.5% vol dissolved in DMF- $\text{Et}_4\text{NBF}_4$  1.0 M). The electrolysis was stopped after 75 C (2.7 F). Usual workup and flash column chromatography (eluent: petroleum ether/ $\text{CH}_2\text{Cl}_2$  50/50,  $R_f=0.7$  in  $\text{CH}_2\text{Cl}_2$ ) gave Diethyl 3,3'-(3,3''',3''''',4''''-tetraoctyl-[2,2':5',2'':5'',2''':5''',2''''':5''''',2''''''-sexithiophene]-5,5''''-diyl)bis(2-cyanoacrylate) D6N as a dark violet solid with yellow metallic reflections in 62% yield.  $^1\text{H}$  NMR ( $\text{CDCl}_3$ )  $\delta$  (ppm): 0.90 (12H, m); 1.31 (40H, m); 1.41 (6H, t,  $J = 7.2 \text{ Hz}$ ); 1.72 (8H, quint,  $J = 7.6 \text{ Hz}$ ); 2.80 (4H, t,  $J = 7.6 \text{ Hz}$ ); 2.86 (4H, t,  $J = 7.6 \text{ Hz}$ ); 4.38 (4H, q,  $J = 7.2 \text{ Hz}$ ); 7.06 (2H, s); 7.15 (2H, d,  $J = 4.0 \text{ Hz}$ ); 7.32 (2H, d,  $J = 4.0 \text{ Hz}$ ); 7.62 (2H, s); 8.23 (2H, s).  $^{13}\text{C}$  NMR ( $\text{CDCl}_3$ )  $\delta$  (ppm): 14.12, 14.25, 22.68, 29.27, 29.29, 29.39, 29.41, 29.47, 29.54, 29.61, 29.67, 30.24, 30.45, 31.86, 31.90, 62.43, 97.71, 116.07, 120.47, 126.18, 126.94, 128.28, 129.13, 132.96, 134.15, 135.36, 138.52, 140.55, 140.80, 141.30, 141.69, 145.98, 163.07.

#### Synthesis of 3,3''',3''''',4'-tetraoctyl-[2,2':5',2'':5'',2''':5''',2''''':5''''',2''''''-sexithiophene]-5,5''''-dicarbaldehyde (BT4F) and 3,4'-dioctyl-[2,2':5',2'':5'',2'''-quaterthiophene]-5-carbaldehyde (BTTF).

$\text{Pd}(\text{PPh}_3)_4$  (2 mol % respect to 5'-bromo-3,4'-dioctyl-[2,2'-bithiophene]-5-carbaldehyde) was added to a solution of 5'-bromo-3,4'-dioctyl-[2,2'-bithiophene]-5-carbaldehyde (0.248 g, 0.5 mmol) and 5,5'-bis(tributylstannyl)-2,2'-bithiophene (0.223

g, 0.30 mmol) in 15 mL of dry toluene under  $\text{N}_2$ , and the mixture was heated to gentle reflux for 24 h. After pouring the mixture into 20 mL of water, the organic phase was extracted with dichloromethane (DCM). The extract was successively washed with water, dried over  $\text{Na}_2\text{SO}_4$  and evaporated in vacuo. The crude product was then purified with column chromatography ( $\text{SiO}_2$ ; hexane) to give 3,3''',3''''',4'-tetraoctyl-[2,2':5',2'':5'',2''':5''',2''''':5''''',2''''''-sexithiophene]-5,5''''-dicarbaldehyde (BT4F) as a dark red oil (0.090 g, 36.0 % yield) and 0.097 g of 3,4'-dioctyl-[2,2':5',2'':5'',2'''-quaterthiophene]-5-carbaldehyde (BTTF) (55.5% yield).

**3,3''',3''''',4'-tetraoctyl-[2,2':5',2'':5'',2''':5''',2''''':5''''',2''''''-sexithiophene]-5,5''''-dicarbaldehyde (BT4F):**  $^1\text{H}$  NMR ( $\text{CDCl}_3$ )  $\delta$  (ppm): 0.88 (6H, m), 0.92 (6H, m), 1.29 (40H, m), 1.65 (4H, m), 2.81 (4H, m), 7.12 (6H, m), 7.58 (2H, s), 9.80 (2H, s).  $^{13}\text{C}$  NMR ( $\text{CDCl}_3$ )  $\delta$  (ppm): 13.69, 14.20, 17.58, 17.63, 20.88, 22.77, 23.93, 26.93, 27.94, 29.36, 29.50, 29.58, 29.80, 30.34, 30.54, 31.98, 124.25, 126.96, 130.50, 132.67, 132.91, 134.60, 137.25, 139.19, 140.16, 140.49, 140.53, 141.18, 182.59.

**3,4'-dioctyl-[2,2':5',2'':5'',2'''-quaterthiophene]-5-carbaldehyde (BTTF):**  $^1\text{H}$  NMR ( $\text{CDCl}_3$ )  $\delta$  (ppm): 0.90 (6H, m), 1.30 (24 H, m), 2.80 (4H, m), 7.05 (3H, m), 7.12 (1H, s), 7.22 (2H, m), 7.56 (1H, s), 9.81 (1H, s).  $^{13}\text{C}$  NMR ( $\text{CDCl}_3$ )  $\delta$  (ppm): 14.14, 22.70, 29.29, 29.36, 29.43, 29.51, 29.54, 30.25, 30.47, 31.90, 123.82, 124.01, 124.70, 126.76, 127.90, 130.34, 132.67, 134.08, 136.86, 137.75, 139.03, 140.03, 140.24, 141.06, 182.37.

#### Synthesis of ethyl 2-cyano-3-(3,4'-dioctyl-[2,2':5',2'':5'',2'''-quaterthiophene]-5-yl)acrylate (BTNN)

To a solution of 0.097 g (0.17 mmol) 3,4'-dioctyl-[2,2':5',2'':5'',2'''-quaterthiophene]-5-carbaldehyde (BTTF) in 20 mL of dry dichloromethane (DCM) were added 0.3 mL of triethylamine. Then 0.177 mL (1.7 mmol,  $d = 1.063 \text{ g mL}^{-1}$ , 10 equiv) of ethyl cyanoacetate were added. The resulting solution was stirred overnight under nitrogen, at room temperature. The reaction mixture was then extracted with dichloromethane (DCM) (2x10 mL), washed with water, then brine and dried over  $\text{Na}_2\text{SO}_4$ . After removal of solvent, the mixture was purified by chromatography on silica gel using ethyl acetate/hexane (1:9) to afford the title compound as a black solid (0.098 g, 88.0 % yield).  $^1\text{H}$  NMR ( $\text{CDCl}_3$ )  $\delta$  (ppm): 0.86 (6H, m), 1.33 (27H, m), 2.80 (4H, m), 4.35 (2H, m), 7.16 (6H, m), 7.90 (1H, s), 8.16 (1H, s).  $^{13}\text{C}$  NMR ( $\text{CDCl}_3$ )  $\delta$  (ppm): 14.1, 22.7, 29.4, 30.0, 30.4, 30.5, 31.9, 62.4, 97.4, 116.0, 123.8, 124.0, 124.7, 126.7, 127.9, 130.7, 132.3, 132.6, 133.2, 134.0, 136.8, 137.8, 140.3, 141.0, 141.8, 145.9, 162.9

#### UV-Vis absorption spectra

Samples for UV and fluorescence measurements were prepared from stock solutions ( $1 \times 10^{-3} \text{ M}$ ) in dichloromethane. The proper volumes of the stock solution were transferred into a vial, then the solvent was evaporated, and the residue dissolved in 2 mL of the suitable solvent. All solutions were equilibrated at 25 °C before each measurement.

UV-Vis investigations were carried out on a Beckman DU 800 spectrophotometer equipped with a Peltier temperature controller. In general, UV-Vis spectra were recorded at 25 °C using a quartz cuvette with a light path of 0.2 cm, at a concentration of  $1 \times 10^{-5}$  M.

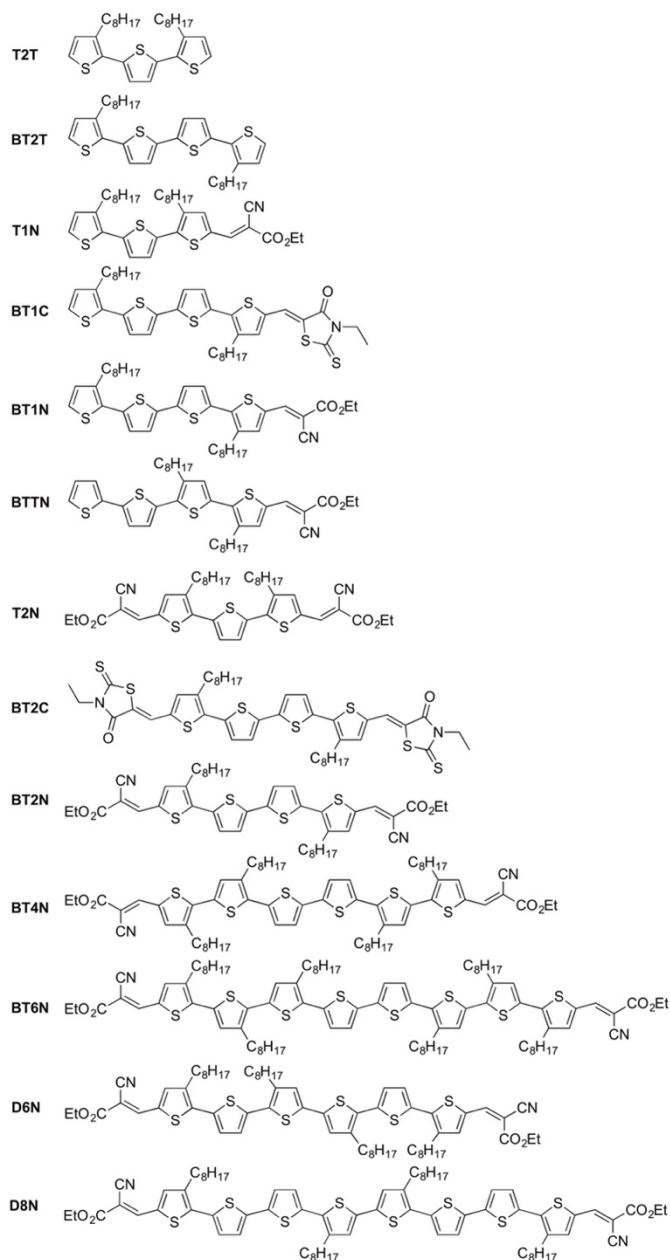
### Fluorescence spectra

Fluorescence measurements were performed at 25 °C on a spectrofluorophotometer (Jasco FP-777W) equipped with a system for temperature control. Emission spectra were recorded at 25 °C, at a concentration of  $1 \times 10^{-5}$  M, using a quartz cuvette with a light path of 0.2 cm in excitation and of 1 cm in emission. The excitation wavelength was chosen on the basis of the  $\lambda_{\text{max}}$  of the relevant absorption spectra. The spectral width was set at 1.5 nm in excitation and 3 nm in emission mode, respectively.

## Results and discussion

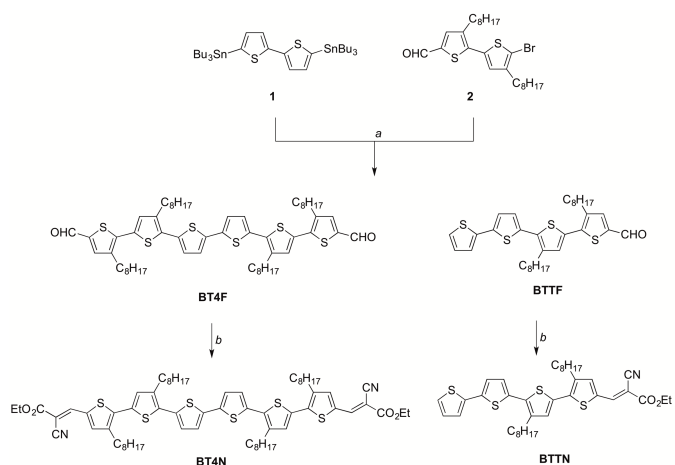
### Electrochemical behaviour

In Figure 1 the structures of all oligothiophenes studied in this work are reported.



Among them the compound **BTTN** was obtained as a by-product during the synthesis of **BT4N** reported in our previous work.<sup>17</sup>

**Figure 1.** Structures of studied oligothiophenes.



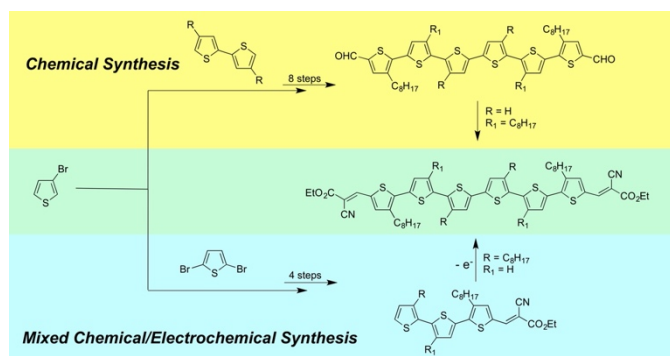
**Scheme 1.** Synthesis of **BT4N** and **BTTN**. Reaction conditions: (a)  $\text{Pd}(\text{PPh}_3)_4$ , toluene; (b) triethylamine, ethyl cyanoacetate, DCM.

The compound **BTTF** is the monosubstituted product of the Stille reaction between compounds **1** and **2**, carried out in presence of tetrakis(triphenylphosphine)-palladium (0) [ $\text{Pd}(\text{PPh}_3)_4$ ] as catalyst and dry toluene as solvent. **BTTF** was obtained with 55% yield.

The Knoevenagel condensation between **BTTF** and ethyl cyanoacetate gave the final product **BTTN**, as a black powder, with 88% yield.

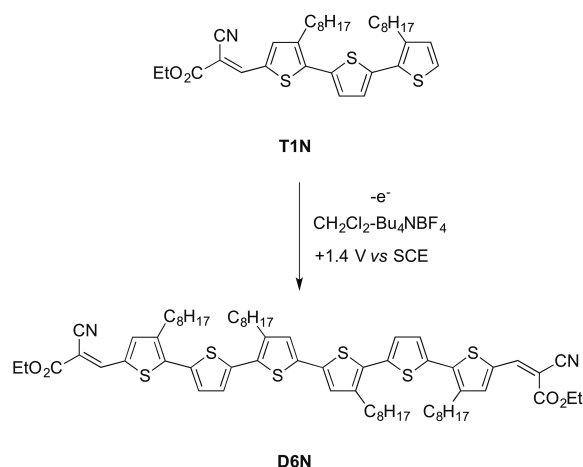
The chemical synthesis of long-chain oligothiophenes, such as **BT4N** and **BT6N** involves many reaction steps, resulting in low overall reaction yields. In addition, toxic organometallic compounds based on nickel and tin are used for some necessary reaction steps, as observed in Scheme 1.

Electrochemistry can be a valid alternative to the classical chemical synthesis to obtain longer oligothiophenes (A-D-A) starting from smaller ones (D-A), decreasing the number of reaction steps and simplifying the synthetic procedure (Scheme 2).



**Scheme 2.** Comparison of chemical and mixed chemical/electrochemical synthesis of long-chain oligothiophenes.

In our previous work<sup>18</sup> the anodic dimerization of **BT1N** was carried out, obtaining the dimer **D8N** with a good yield. Although we had no information about the application of this electrochemical dimerization to different substrates, this same procedure was successfully applied to **T1N**, precursor of **D6N** (Scheme 3).



**Scheme 3.** Anodic dimerization of **T1N**.

The electrolysis was performed in a divided glass cell on a solution of  $\text{CH}_2\text{Cl}_2$ - $\text{Bu}_4\text{NBF}_4$  0.1 M containing **T1N**, at 25 °C, under nitrogen atmosphere using Pt electrodes. Potentiostatic conditions were chosen to carry out the experiment, by setting the value of +1.4 V (vs mSCE). The electrolysis was stopped after the consumption of 2.7 F and the usual workup gave **D6N** in 62% yield. The excellent result obtained was not entirely predictable and it confirmed the possibility of applying the electro synthetic methodology even starting from smaller (three thiophene units) D-A oligothiophenes than **BT1N** (four thiophene units).

The obtained **D6N** can be considered a structural analogous of **BT4N**, as well as **D8N** is for **BT6N**. In fact, they have the same number of thiophene units but different positions of alkyl chains.

By means of cyclic voltammetry, the electrochemical behaviour of **D6N** has been studied (Figure 2) and then compared with that of **BT4N**.

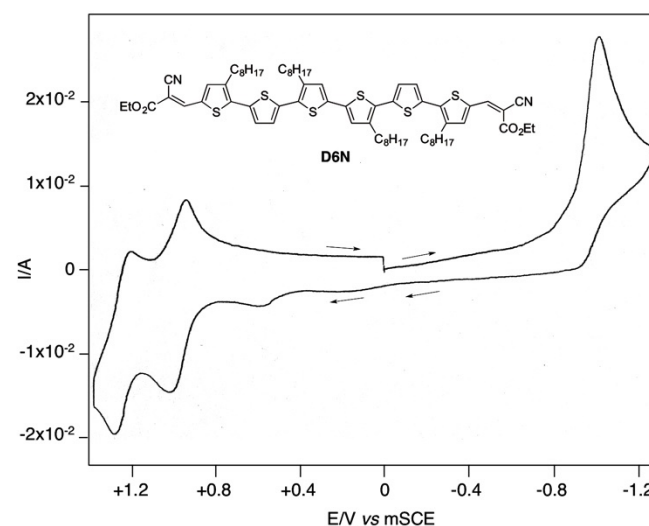


**Figure 2.** Cyclic voltammogram of **D6N**  $1 \times 10^{-2}$  M in  $\text{CH}_2\text{Cl}_2$ - $\text{Bu}_4\text{NBF}_4$  0.1 M. Working electrode: GC. Reference electrode: mSCE.  $v = 0.1 \text{ V s}^{-1}$ ,  $T = 25^\circ\text{C}$ . Potential scan: 0.0 to -1.3 to +1.4 to 0.0 V.

The first oxidation peak of **D6N** is reversible and it has a potential value of +1.00 V vs mSCE, higher than the **BT4N** data

(+0.94 V). On the other hand, the cathodic peak of **D6N** (-1.01 V) and **BT4N** (-1.04 V) are similar. The different position of the alkyl chains on the thiophene backbone has therefore influenced the oxidation process, leaving almost unchanged the reduction one, as expected considering the donor effect of the octyl groups.

Cyclic voltammetry is useful also to obtain the energy levels of target compounds and then the electrochemical band gaps. As seen in a previous work,<sup>18</sup> **D8N** showed a lower bandgap than **BT6N**. The same comparison can be carried out with the six-units oligothiophenes: **D6N** and **BT4N**. Again, a lower band gap is observed for the electrodimersized oligothiophene **D6N** ( $E_{g(\text{BT4N})} = 1.78 \text{ eV}$  vs  $E_{g(\text{D6N})} = 1.72 \text{ eV}$ ).

### Solvatochromic investigation

As soon as all the studied compounds are dissolved in dichloromethane (DCM), they reveal their different response to the nature of the solvent, as accounted for by different colours exhibited by the solutions obtained (Figure 3a). Furthermore, when irradiated at 368 nm, they also gave emission of different colours (Figure 3b).

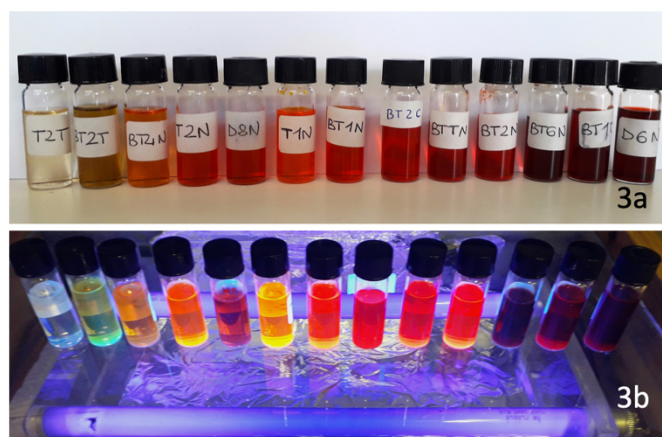


Figure 3. Colour shades of: a) DCM solutions of oligothiophenes; b) irradiated at 368 nm.

To have more insights about the effect of the solvent nature on the photophysical properties of oligothiophenes, UV-Vis and emission spectra were recorded in different solvents. In particular, aprotic solvents having different polarity, like cyclohexane (Cy), chloroform ( $\text{CHCl}_3$ ), toluene (Tol), dichloromethane (DCM), acetonitrile (ACN) and ethyl acetate (AcOEt) were used, and the data are presented in Table 1.

Table 1. Absorption data of compounds in all studied solvents.  $C=1 \times 10^{-5} \text{ M}$ .  $\lambda_{\text{max}}$  absorption (nm). <sup>a</sup>Low solubility.

|             | DCM | $\text{CHCl}_3$ | ACN              | AcOEt            | Cy               | Tol |
|-------------|-----|-----------------|------------------|------------------|------------------|-----|
| <b>T2T</b>  | 338 | 338             | 337              | 335              | 332              | 338 |
| <b>BT2T</b> | 382 | 383             | 375              | 375              | 369              | 376 |
| <b>T1N</b>  | 448 | 452             | 437              | 437              | 432              | 446 |
| <b>T2N</b>  | 470 | 471             | 463              | 462              | 439              | 467 |
| <b>BT1C</b> | 484 | 495             | 472              | 477              | 474              | 484 |
| <b>BT1N</b> | 452 | 464             | 444              | 439 <sup>a</sup> | 446              | 459 |
| <b>BT2C</b> | 505 | 511             | 484 <sup>a</sup> | 474              | 459 <sup>a</sup> | 495 |
| <b>BT2N</b> | 486 | 492             | 462              | 469              | 455              | 484 |
| <b>BTTN</b> | 455 | 464             | 439              | 440              | 442              | 457 |
| <b>BT4N</b> | 445 | 438             | 426              | 421              | 432              | 444 |
| <b>BT6N</b> | 484 | 484             | 412 <sup>a</sup> | 457              | 461              | 476 |
| <b>D6N</b>  | 484 | 490             | insoluble        | 470              | 460              | 481 |
| <b>D8N</b>  | 484 | 493             | 449              | 461              | 450              | 485 |

Superimposed UV-vis spectra, recorded for **BT1C** in different solvents are shown in Figure 4. Spectra corresponding to all the other oligothiophenes are displayed in Figures A1-A13 (Electronic Supplementary Information).

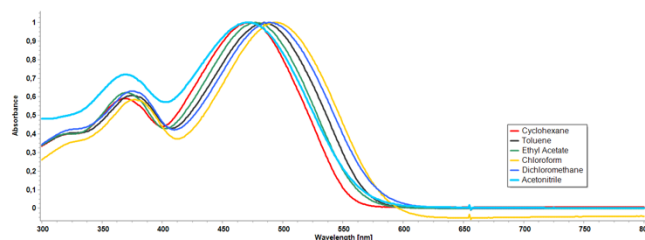


Figure 4. UV-Vis spectra of **BT1C** in different solvents

Analysis of the above spectra sheds light on the significant effect that solvent nature exerts on the position of the main absorption band. In particular, it was firstly bathochromically shifted going from cyclohexane to  $\text{CHCl}_3$ , but it exhibited a hypsochromic shift with the further increase in solvent polarity. With the only exception of **T2T**, a similar behaviour was detected for all the other oligothiophenes studied in this work. In the attempt to correlate the above trend to solvent polarity, we plotted the position of the main absorption band ( $\lambda_{\text{abs}}$ ) as a function of  $E_{\text{T}}(30)$  values (Figure 5 for **BT1C** and Figures A14-A20 for all other oligothiophenes). This parameter accounts for solvent polarity, measuring the effect on the transition energy for the longest-wavelength solvatochromic absorption band of the pyridinium N-phenoxide betaine dye.<sup>20</sup>

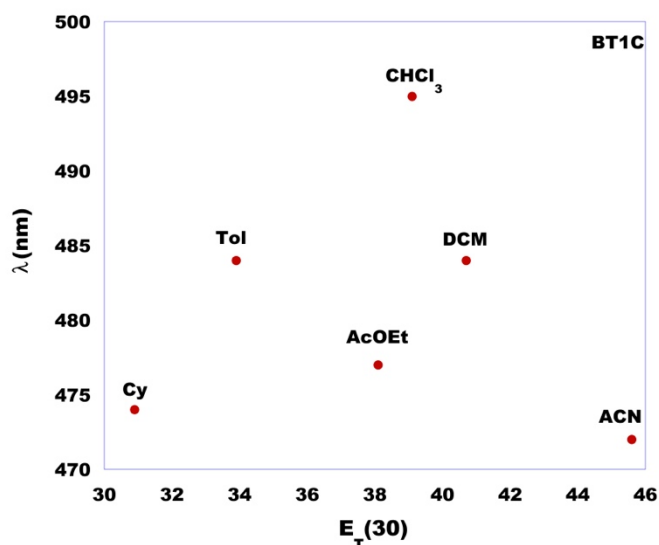


Figure 5. Trend of  $\lambda_{\text{abs}}$  of BT1C as a function of solvent polarity,  $E_{\text{T}}(30)$ .

In almost all cases considered, we obtained bell shaped curves showing the maximum value in correspondence of  $\text{CHCl}_3$  solution. Only in the case of T2T,  $\lambda_{\text{abs}}$  was bathochromic ally shifted, going from Cy to Tol, but it remained unchanged with the further increase in solvent polarity (Figure A1).

Among all tested solvents, only in solution of AcOEt, we obtained  $\lambda_{\text{abs}}$  values lower than the ones detected in solvents having comparable polarity.

Analysis of data previously reported in literature allows stating that the above behaviour can be ascribed to the occurrence of a solvatochromism inversion process.<sup>21-23</sup>

The mechanism of this process is not fully understood. The most corroborated hypothesis suggests the presence of degenerated electronic states with different electronic distribution, that gives the same absorption band as a result of a superimposition process. The solvatochromism inversion is detected only if two bands exhibit different solvatochromic shift and absorption coefficients are differently affected by solvent polarity.<sup>23</sup> Effects of solvatochromism inversion are classified as weak or strong, if shifts lower than 20 nm or higher than 100 nm are detected, respectively.

In the majority of cases analysed in this work, solvatochromic effects detected for oligothiophenes proved weak and the weakest ones were obtained for T2T, BT2T and BT4N.

In the attempt to better analyse obtained results, we discerned the positive solvatochromism effect (bathochromic shift) from the negative ones (hypsochromic shift) (Figure 6).

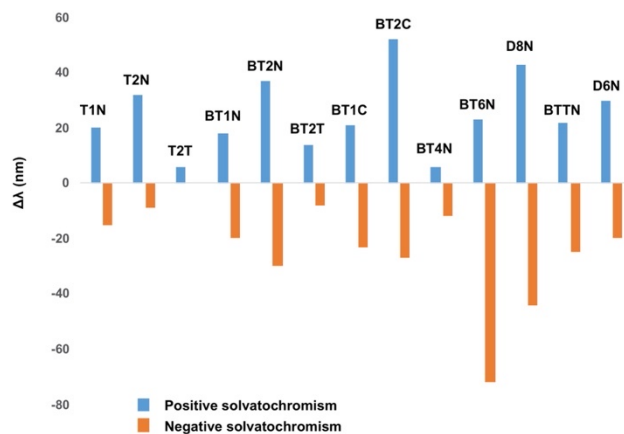


Figure 6. Positive and negative solvatochromism effects for different oligothiophenes.

We observed moderate positive effects for T2N and BT2N, and more pronounced effects for BT2C and D8N. Differently, negative solvatochromic effects were less significant than the corresponding positive ones, and only in the cases of BT6N and D8N, we observed shifts higher than 30 nm. In general, the most significant solvatochromic effects were detected for symmetrically substituted oligothiophenes (BT2N and BT2C), with the higher shift measured when the  $\pi$ -conjugated system ended with the heterocyclic unit (BT2C>BT2N).

As far as the central unit is concerned, analysis of collected data shows that the elongation of the  $\pi$ -conjugated system firstly weakens the effect and subsequently strengthens it, as accounted for the observed trend in positive solvatochromism (BT2N>BT4N<BT6N). The above hypothesis is perfectly supported as far as data for BT2N and D8N are compared. Indeed, in the above cases, the elongation of  $\pi$ -conjugated systems exerts a significant increase in both positive and negative solvatochromism.

Solvatochromic effects were also investigated recording emission spectra (Figures A21-A33). The emission peak data are summarized in Table 2.

Table 2. Fluorescence emission data of compounds in all studied solvents.  $C=1 \times 10^{-5}$  M.  $\lambda_{\text{max}}$  emission (nm). Low peak intensity is indicated with "low".

|      | DCM     | $\text{CHCl}_3$ | ACN     | AcOEt   | Cy      | Tol     |
|------|---------|-----------------|---------|---------|---------|---------|
| T2T  | 436     | 435             | 428     | 431     | 435     | 435     |
| BT2T | 457-484 | 456-487         | 455-479 | 452-480 | 453-480 | 456-485 |
| T1N  | 582     | 576             | 602     | 566     | 513-542 | 545     |
| T2N  | 571     | 569             | 576     | 561     | 538-575 | 545     |
| BT1C | 648     | 643             | 657     | 619     | 559     | 595     |
| BT1N | 626     | 614             | 643     | low     | 542     | 585     |
| BT2C | 640     | 638             | low     | 623     | low     | 609     |
| BT2N | 609     | 601             | 621     | 594     | 559     | 585     |
| BTTN | 624     | 620             | 647     | 610     | 548-577 | 587     |
| BT4N | 592     | 597             | 577     | 587     | 570     | 588     |
| BT6N | 640     | 640             | low     | 631     | 589     | 619     |
| D6N  | 655     | 645             | low     | 627     | 585     | 611     |
| D8N  | 655     | 654             | low     | 635     | 582     | 609     |

In general, the emission behaviour was more significantly affected by solvent nature than absorption one. In some cases, it was not possible to obtain the emission data, due to the poor solubility of the oligothiophenes in some solvents used for emission spectroscopy compared to absorption one. In Figure 7 the **BTTN** emission spectra, recorded in all studied solvents, are reported as example.

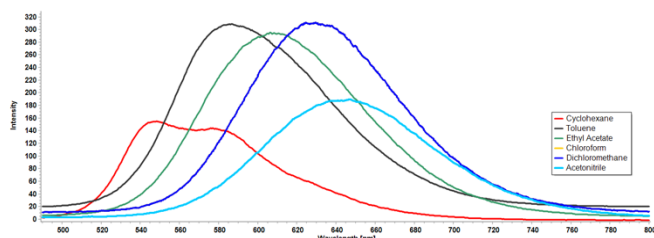


Figure 7. Emission spectra of **BTTN** in all studied solvents

Also in this case, we analysed the position of the main emission band as a function of solvent polarity, evidencing the occurrence of solvatochromism inversion only in the case of **BT4N**, differently from the UV-Vis investigation, which did not show solvatochromism inversion for **BT4N** (Figure 8).

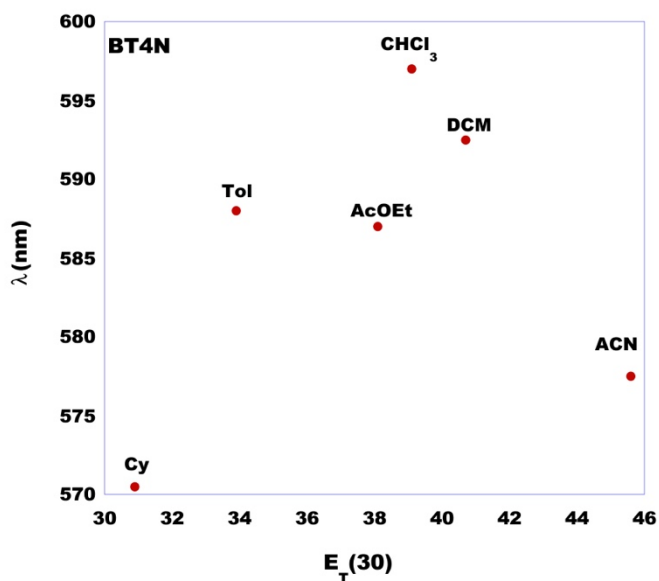


Figure 8. Trend of  $\lambda_{em}$  of **BT4N** as a function of solvent polarity,  $E_T(30)$ .

All other oligothiophenes exhibited positive solvatochromism effects (Figures A34-A40). The **BTTN** trend of  $\lambda_{em}$  is reported in Figure 9, taken as an example to illustrate the general emission trend of all oligothiophenes.

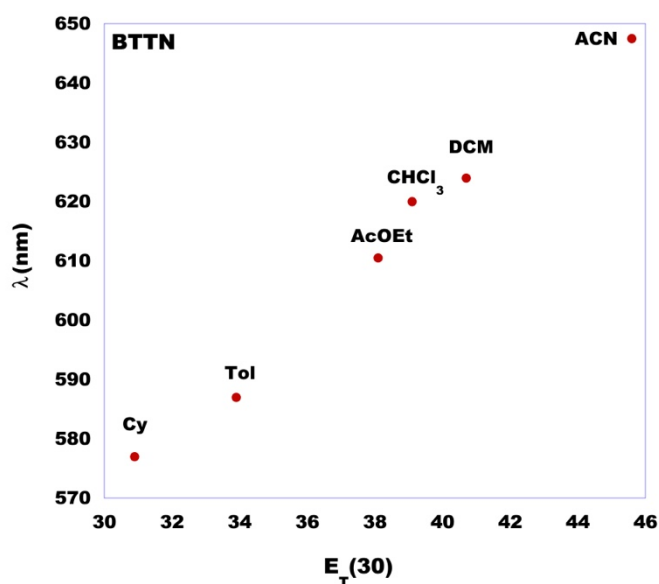


Figure 9. Trend of  $\lambda_{em}$  of **BTTN** as a function of solvent polarity,  $E_T(30)$ .

It is possible to observe a linear bathochromic shift that occurs increasing the polarity of the solvent. With only a few exceptions, in the case of the emission spectroscopy, the solvatochromic effects were significant with bathochromic shift going from 40 up to 100 nm (Figure 10).

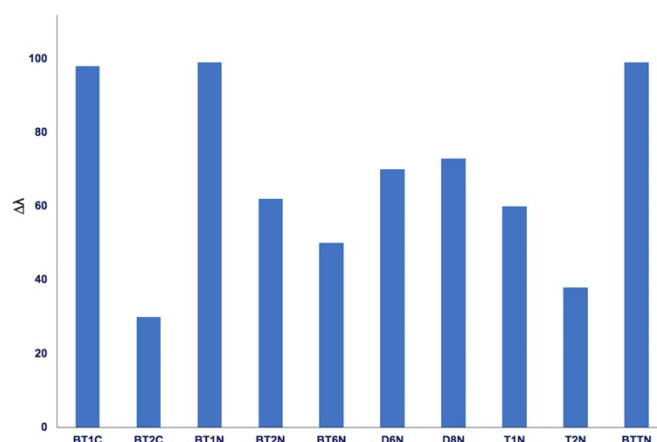


Figure 10. Positive solvatochromism effect for different oligothiophenes.

A deep analysis of above data, evidence that extending the  $\pi$ -conjugated system has a different effect depending on the elongation nucleus. Indeed, it induces a drop in the effect as far as the 3-octylthiophene nucleus is concerned (**BT2N** and **BT6N**); whereas the measured effect remains unchanged if the elongation nucleus is the thiophene ring (**D6N** and **D8N**). Furthermore, the entity of the effect depends on the symmetrical or unsymmetrical oligothiophene substitution, proving more significant in the latter than in the first case, as accounted for by the comparison between **BT1C** and **BT2C**,

**BT1N** and **BT2N**, **T1N** and **T2N**, with the more significant difference detected in the first case.

Data collected were also analysed by using the Lippert-Mataga equation,<sup>24</sup> to assess the sensitivity of the studied oligothiophenes to changes in solvent polarity. In particular, the Lippert-Mataga equation accounts for the correlation between the Stokes shift ( $\Delta\nu_f$ ) and orientation polarizability ( $\Delta f$ ), according to eqs (1) and (2):

$$\Delta\nu_f = 2 (\mu_e - \mu_g)^2 \Delta f h c a^3 + C \quad (1)$$

where  $\mu_e$  and  $\mu_g$  are the dipole moment corresponding to the excited and ground state,  $h$  is Planck's constant,  $c$  is the speed of light in vacuum,  $a$  is the radius of the cavity containing the fluorophore and  $\Delta f$  is given by eq. (2):

$$\Delta f = [(\epsilon-1)/(2\epsilon+1)] - [(n^2-1)/(2n^2+1)] \quad (2)$$

where  $n$  and  $\epsilon$  represent the refraction index and dielectric constant of the solvent.

The occurrence of a linear correlation allows stating that the solvatochromic behaviour can be only ascribed to changes in solvent polarity and ruling out the occurrence of specific solute-solvent interactions.

In our case, good linear correlations were obtained only for **T2T**, **BT1C**, **BT1N**, **BT2N** and **T2N** (Figures A41-A47). With the only exception of **T2T** in all the other cases the slope of the linear correlation was positive, indicating that the increase in solvent polarity induces a more significant stabilization of the excited state with respect to the ground state.

Slopes of the linear correlations change along the following trend: **T2T**<**T2N**<**BT1C**≈**BT1N** (Table A1). Analysis of the above trend shows that the increase in the  $\pi$ -conjugated system, going from **T2T** to **BT1C** and **BT1N**, induces a significant increase in the chromophore sensitivity to the solvent polarity. On the other hand, comparison between data obtained for **BT1C** and **BT1N** evidence that, in the presence of an unsymmetrical substitution, the above parameter is not affected by the nature of the substituent.

Finally, according to the analysis of positive solvatochromism effects detected by recording emission spectra, the symmetrical substitution of the  $\pi$ -conjugated system induces a drop in sensitivity to solvent polarity, as accounted for by the comparison between slopes corresponding to **T1N** and **T2N**.

## Conclusions

We synthesized a series of push-pull oligomers based on thiophene and bithiophene cores, both by chemicals and electrochemical syntheses and here we report a detailed analysis on the observed solvatochromic effects on solutions of these compounds realized with a number of solvents with different polarities. The solvatochromism study was carried on by the analysis of the UV-Vis absorption and fluorescence spectra of these solutions that are related, in a close relationship, with the polarity of the solvent, to several factors related to the studied compounds as their D-A or A-D-A

structures, the number of thiophene units, the position (and number) of alkyl chains in the backbone, and, finally, the type of acceptor end-groups. Oligothiophenes synthesis has been improved by means of anodic dimerization of shorter precursors. Electrochemical synthesis of new donor-acceptor oligothiophenes are currently under development in our laboratory, with the dual purpose of obtaining compounds with increasingly better performances for applications in the field of organic electronics and to demonstrate how anodic electro-dimerization can be an excellent tool for the synthesis of long-chain oligothiophenes in a cleaner and more efficient way.

## Conflicts of interest

There are no conflicts to declare.

## Acknowledgements

The authors acknowledge Sapienza University of Rome for financial support and Mr. Marco Di Pilato for his help with the voltammetric analysis.

## References

- H. Klauk, *Organic Electronics: Materials, Manufacturing and Applications*, Wiley-VCH, Weinheim, 2006.
- H. Klauk, *Organic Electronics II: More Materials and Applications*, Wiley-VCH, Weinheim, 2012.
- P. Bäuerle, J. Becher, J. Lau and P. Mark, in *Electronic Materials: The Oligomer Approach*, ed. K. Müllen and G. Wegner, Wiley-VCH, Weinheim, 1998, 2, 105–233.
- J. Pei, J. L. Wang, X. Y. Cao, X. H. Zhou and W. B. Zhang, *J. Am. Chem. Soc.*, 2003, **125**, 9944.
- X. M. Li, J. Zhang, G. L. Huanga, Y. F. Wang, M. Z. Rong, M. Y. Teng and J. Liu, *Dyes Pigm.*, 2017, **141**, 1.
- J. S. Cho, Y. Kojima and K. Yamamoto, *Polym. Adv. Technol.*, 2003, **14**, 52.
- M. E. Cinar and T. Ozturk, *Chem. Rev.*, 2015, **115**, 3036.
- R. B. K. Siram, K. Tandy, M. Horecha, P. Formanek, M. Stamm, S. Gevorgyan, F. C. Krebs, A. Kiriy, P. Meredith, P. L. Burn, E. B. Namdas and S. Patil, *J. Phys. Chem. C*, 2011, **115**, 14369.
- C. Zhang and X. Zhu, *Acc. Chem. Res.*, 2017, **50**, 1342.
- Q. Zhang, B. Kan, F. Liu, G. Long, X. Wan, X. Chen, Y. Zuo, W. Ni, H. Zhang, M. Li, Z. Hu, F. Huang, Y. Cao, Z. Liang, M. Zhang, T. P. Russell and Y. Chen, *Nature Photon.*, 2015, **9**, 35.
- Z. Li, G. He, X. Wan, Y. Liu, J. Zhou, G. Long, Y. Zuo, M. Zhang and Y. Chen, *Adv. Energy. Mater.*, 2012, **2**, 74.
- Y. Chen, X. Wan and G. Long, *Acc. Chem. Res.*, 2013, **46**, 2645.
- B. Kan, M. Li, Q. Zhang, F. Liu, X. Wan, Y. Wang, W. Ni, G. Long, X. Yang, H. Feng, Y. Zuo, M. Zhang, F. Huang, Y. Cao, T. P. Russell and Y. Chen, *J. Am. Chem. Soc.*, 2015, **137**, 3886.
- K. Lim, M. S. Kang, Y. Myung, J. H. Seo, P. Banerjee, T. J. Marks and J. Ko, *J. Mater. Chem. A*, 2016, **4**, 1186.
- L. Salamandra, L. La Notte, G. Paronesso, G. Susanna, L. Cinà, G. Polino, L. Mattiello, A. Catini, C. Di Natale, E. Martinelli, A. Di Carlo, F. Brunetti, T. M. Brown and A. Reale, *Energy Technol.*, 2017, **5**, 2168.
- O. D. Parashchuk, A. A. Mannanov, V. G. Konstantinov, D. I. Dominskiy, N. M. Surin, O. V. Borshchev, S. A. Ponomarenko, M. S. Pshenichnikov and D. Y. Paraschuk, *Adv. Funct. Mater.*, 2018, **28**, 1800116.



- 17 F. Pandolfi, D. Rocco and L. Mattiello, *Org. Biomol. Chem.*, 2019, **17**, 3018.
- 18 M. Feroci, T. Civitarese, F. Pandolfi, R. Petrucci, D. Rocco, D. Zane, G. Zollo and L. Mattiello, *ChemElectroChem*, 2019, **6**, 4016.
- 19 P. W. Carr, *Microchem. J.*, 1993, **48**, 4.
- 20 T. W. Bentley, F. L. Schadt, and P. v. R. Schleyer, *J. Am. Chem. Soc.*, 1972, **94**, 992.
- 21 Y. Lim, E. Lee, Y. R. Yoon, M. S. Lee and M. Lee, *Angew. Chem., Int. Ed.*, 2008, **47**, 4525.
- 22 P. Jacques, *J. Phys. Chem.*, 1986, **90**, 5535.
- 23 H. Tamaya, Y. Torii, T. Ishikawa, H. Nakano and T. Iimori, *ChemPhysChem*, 2019, **20**, 2531.
- 24 S. Sumalekshmy and K. R. Gopidas, *J. Phys. Chem. B*, 2004, **108**, 3705.